



Best practices and methods

Revisiting the binary azeotropic separation containing tetrahydrofuran and ethanol: Design and control of extractive distillation using dimethyl sulfoxide as alternative solvent

Zong Yang Kong^a, Ao Yang^{b,c,*}, Agus Saptoro^{d,**}, Jaka Sunarso^a^a Research Centre for Sustainable Technologies, Faculty of Engineering, Computing and Science, Swinburne University of Technology, Jalan Simpang Tiga, Kuching, Sarawak 93350, Malaysia^b College of Safety Engineering, Chongqing University of Science and Technology, Chongqing 401331, PR China^c Chongqing Key Laboratory for Oil and Gas Production Safety and Risk Control, Chongqing 401331, PR China^d Department of Chemical and Energy Engineering, Curtin University Malaysia, CDT 250 Miri, Sarawak 98009, Malaysia

ARTICLE INFO

Keywords:

Extractive distillation
Azeotropic separation
Process control
Energy-saving
Resource conservation

ABSTRACT

This study reexamined the possibility of improving the separation of binary azeotropic mixture containing tetrahydrofuran (THF) and ethanol from previous work (*J Chem Technol Biotechnol* 2015; 90: 1463–1472) that rely on the extractive distillation (ED) using ethylene glycol (EG) as solvent. Here, dimethyl sulfoxide (DMSO) is proposed as an alternative solvent for the ED, and its feasibility is preliminary screened and compared against the usage of EG. The conceptual ED using DMSO is designed by manipulating all the design variables until the minimum product specifications (i.e. purity) are achieved. Then, the conceptual design is further optimised using particle swarm algorithm to obtain the ideal column configuration and the performance is compared against the ED using ethylene glycol (EG) and pressure swing distillation (PSD) (i.e. best process) from previous work based on economic and CO₂ emission. Overall, the optimised ED using DMSO provides 36% and 37% lower economic and CO₂ emission with respect to the ED using EG. In comparison to PSD (i.e. best process) from previous work, it provides 24% and 25% reduction in TAC and CO₂ emission. Lastly, a control structure is developed for the proposed ED using DMSO that can effectively handle $\pm 10\%$ throughput and $\pm 5\%$ feed composition disturbances without the need of a composition controller as in the case of previous work.

1. Introduction

Tetrahydrofuran (THF) is commonly employed as organic solvent in the chemical industries such as for the manufacturing of adhesives and polyvinyl chloride (PVC). It is also an important raw material for the production of adipic acid. Ethanol, on the other hand, is commonly used in the pharmaceutical industries such as for the manufacturing of drugs and medicines. In addition, both THF and ethanol are sustainable biomass energy sources (Luis et al., 2014; Wang et al., 2015a). Therefore, the recovery of these two valuable components help to safeguard the environmental and facilitate a sustainable resource recovery process. One common source of THF–ethanol mixtures is the synthesis of a liquid crystal monomer (Wang et al., 2015a) or from the norgestrel manufacturing process (Zhao et al., 2017a). However, the mixture of THF and ethanol forms a minimum-boiling azeotrope in the binary system when the mole fraction of THF is 0.8582 at atmospheric pressure. The azeotropic mixture complicates the separation process between the in-

dividual components, meaning that the azeotropic mixture cannot be effectively separated by using ordinary distillation process. Several other distillation-based techniques have been devised such as extractive distillation (ED) (Yang et al., 2022b), pressure swing distillation (PSD) (Yang et al., 2022a), or the recently emerging hybrid reactive-extractive distillation (Kong et al., 2022b, 2022c; Yang et al., 2023) to overcome this bottleneck.

Today, our literature survey has revealed that there is an increasing interest on the recovery and separation process of THF and ethanol, as reflected by the increasing number of publications in the last 7 years (Li et al., 2019; Su et al., 2020; Tang et al., 2013; Wang et al., 2015a, 2015b; Yang et al., 2020, 2019; Zhang et al., 2019, 2018; Zhang et al., 2021; Zhao et al., 2018, 2017b, 2017a). Majority of these studies rely on the ED while a few studies relied on the PSD for the separation and recovery of THF and ethanol. These studies are categorised according to the binary and ternary azeotropic mixture that contains THF and ethanol in Fig. 1, the details of which are covered in our previous review paper

* Corresponding author at: College of Safety Engineering, Chongqing University of Science and Technology, Chongqing 401331, PR China.

** Co-corresponding author at: Department of Chemical and Energy Engineering, Curtin University Malaysia, CDT 250 Miri, Sarawak 98009, Malaysia.

E-mail address: skzyang@outlook.com (Z.Y. Kong).

Nomenclature

ED	extractive distillation
EG	ethylene glycol
EDC	extractive distillation column
DMF	dimethylformamide
DMAC	dimethylacetamide
GA	genetic algorithm
IMC	internal model control
MINLP	mixed integer nonlinear programming problem
MADS	mesh adaptive direct search
NHV	net heating value
PSD	pressure swing distillation
PSO	particle swarm optimisation
PP	payback period
PVC	polyvinyl chloride
SRC	solvent recovery column
SI	sequential iteration
SQP	sequence quadratic programming
SA	simulated annealing
SVD	singular value decomposition
THF	tetrahydrofuran
TAC	total annual cost
TCC	total capital cost
TOC	total operational cost

(Alcántara Avila et al., 2021; Kong et al., 2022a). For the studies that worked on ternary azeotropic mixture, the third component is water since all these existing studies focused on recovery of THF and ethanol from waste effluent. For each category (i.e. binary or ternary), we further classify them based on design and control studies. From Fig. 1, it becomes apparent that most of the existing studies primarily focused on the ternary azeotropic mixture, with only three that worked on the binary

azeotropic mixture of THF and ethanol (Tang et al., 2013; Wang et al., 2015b, 2015a). Moreover, majority (i.e. 10 out of 13) studies had prioritised (i.e. worked) on the steady-state design without exploring much on the control performance of the separation process. To this end, this study aims to focus on both the steady-state design and control performance of the ED for the separation and recovery of binary azeotropic mixture containing THF and ethanol.

In this study, we wish to revisit the previous work that rely on the ED using ethylene glycol (EG) as solvent (Wang et al., 2015a) because we realised that there are some interesting observations and hypotheses that can further improve the separation process performance. In previous study, Wang et al. (2015a) assessed the performance of the ED using EG and PSD for the separation of THF and ethanol in terms of total annual cost (TAC). From their steady-state simulation, it was revealed that the PSD provides a lower TAC in comparison to the ED using EG. In the following year, Wang's research group also extended the study by comparing the control performance of both PSD and ED using EG, to ensure that there is no trade-off between economical and control performances (Wang et al., 2015b). Relative to the ED using EG, the PSD can return the products purities back to their original specification more quickly and therefore, resulted in a better control performance. However, both the ED and PSD rely on the usage of composition controller for maintaining the two products purities at their desired specification, which is expensive and difficult to maintain in the industry.

Contrary to previous work (Wang et al., 2015a, 2015b), the main contribution of this work is to explore an alternative solvent for the ED that provides a more economical and environmentally friendly separation process for the separation of binary azeotropic mixture containing THF and ethanol. Other than steady-state design, another contribution of this work is to develop a control structure for the proposed ED using the alternative solvent that provides similar control performance without the need of a composition controller.

The remainder of this paper is organised as follows. First, the ED using EG from previous work is described in Section 2 to provide our readers with a clear understanding of the process. Section 3 explains

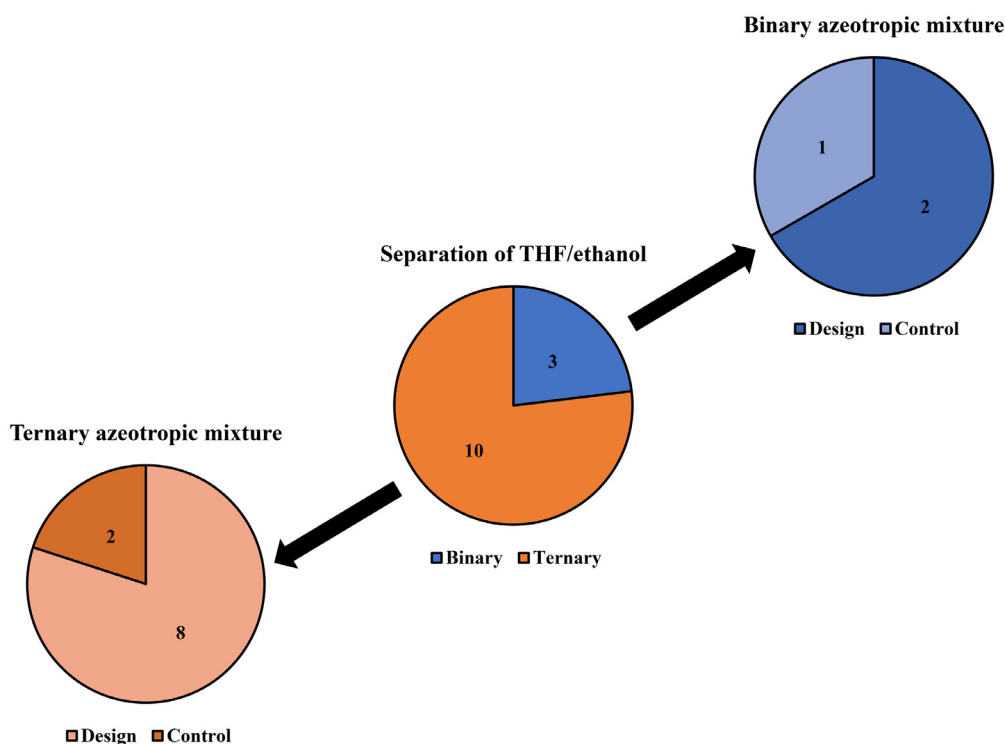


Fig. 1. Summary of recent studies on separation of THF/ethanol.

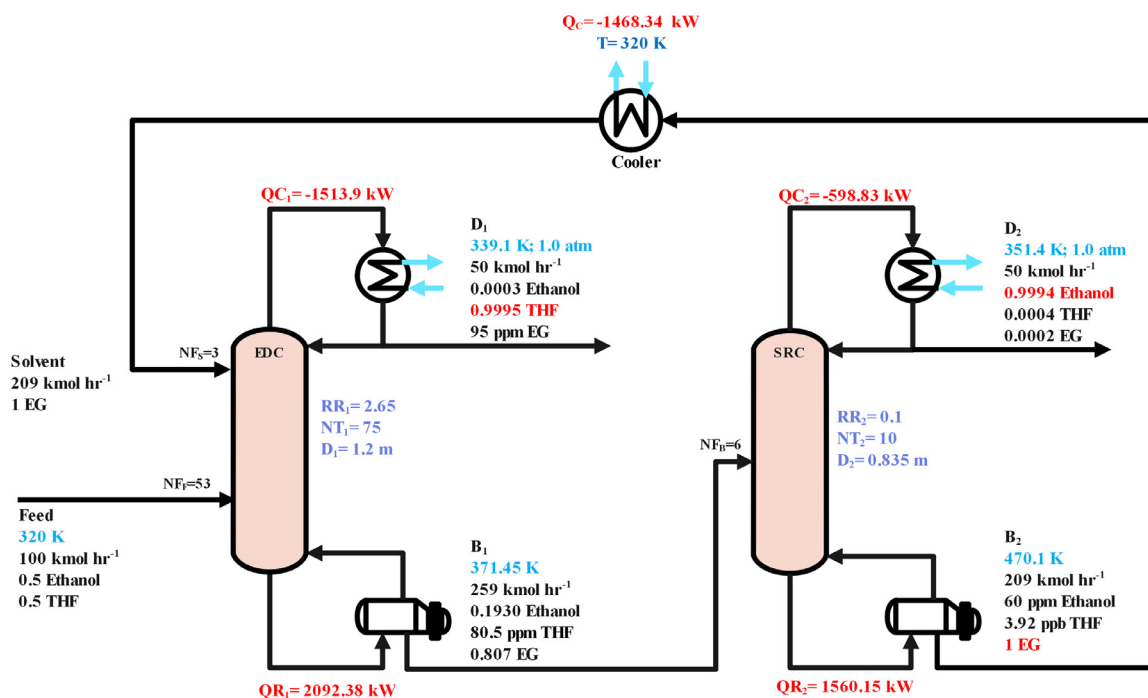


Fig. 2. ED using EG (Reproduced from Wang et al. (2015a)).

the methodology that includes the solvent screening, conceptual design, process optimisation, process evaluation, and dynamic simulation. The simulation results are elucidated in Section 4 while Section 5 wrap up this study by providing recommendations for future work.

2. Extractive distillation using ethylene glycol

Fig. 2 shows the ED using EG for the separation of THF and ethanol reproduced from the work of Wang et al. (2015a). Here, the percentage difference in the TAC between the reproduced ED (Fig. 2) and previous work is less than 5%, which reflects the reliability of our reproduced model. The fresh feed stream enters the extractive distillation column (EDC) together with the EG as solvent, which facilitates the binary azeotropic separation between THF and ethanol. The high purity THF is obtained from the distillate of EDC while the remainder mixture containing ethanol and EG solvent are obtained from the bottom of the EDC and is directed to the solvent recovery column (SRC) for subsequent solvent regeneration. In the SRC, high purity ethanol is obtained from the distillate while the regenerated (i.e. recovered) EG solvent is obtained at the bottom and cooled before it is recycled back to the EDC.

3. Methodology

The work procedure of this study is arranged as follows: Firstly, we reproduced the ED using EG from the work of Wang et al. (2015a), which will be used as base case for subsequent comparison against the proposed ED using the alternative solvent. Next, a suitable alternative solvent is selected to replace EG solvent in the base case using ternary diagram and residue curve map(s). Then, we conceptually develop the ED using the alternative solvent by manipulating the design variables until the minimum product specifications (i.e. purity) can be met. Following this, the conceptual (i.e. initial) design of the proposed ED is optimised to obtain the optimum column configuration. The performance of the optimised ED using alternative solvent is compared against the ED using EG and the PSD (i.e. best process) from previous work based on the economic and environmental perspectives, which are represented using TAC and CO₂ emission. Lastly, we also proposed a control structure for

the ED using the alternative solvent without the use of the composition controllers and the control performance is also compared against the base case. Fig. 3 graphically summarised the methodology used in this work.

3.1. Solvent screening

Fig. 4 shows the ternary diagram for the binary azeotropic mixture containing THF and ethanol with the solvent (S) that belongs to the Serafimov's class 1.0–1a (Gerbaud et al., 2019). In Fig. 4, the uni-volatility line (i.e. red dash line) in between two components (i.e. THF and solvent S) is marked as x_p , which is used to evaluate the efficiency of the different solvent. The solvent with a smaller value of x_p (i.e. intersection point closer to the target component) generally represent a lower amount of solvent flowrate required, which translates to lower TAC. Here, we only compared the performance between using EG and DMSO for the binary azeotropic separation of THF and ethanol because previous studies have shown that these two solvents are better than some of the commonly used solvents for ED such as dimethylformamide (DMF) and dimethylacetamide (DMAC) (Chen et al., 2022; Zhao et al., 2017b).

3.2. Conceptual design

Once the suitable solvent has been selected, the conceptual ED is designed by varying the design variables until all the design specifications can be met. The design variables used in this work include the total stages in both EDC and SRC, locations of feed and solvent inlet, distillate rate, reboiler duty, reflux ratio, and solvent flowrate. These design variables are commonly used by the existing studies in this area (Chen et al., 2022; Wang et al., 2012). The ED is simulated using Aspen Plus V11 and UNIQUAC was used as the thermodynamic package (Table S1), identical to previous work (Wang et al., 2015a). The fresh feed flowrate is 100 kmol hr⁻¹, which contains equimolar of THF and ethanol. The desired product purities for the THF and ethanol are both 99.9 mol.%.

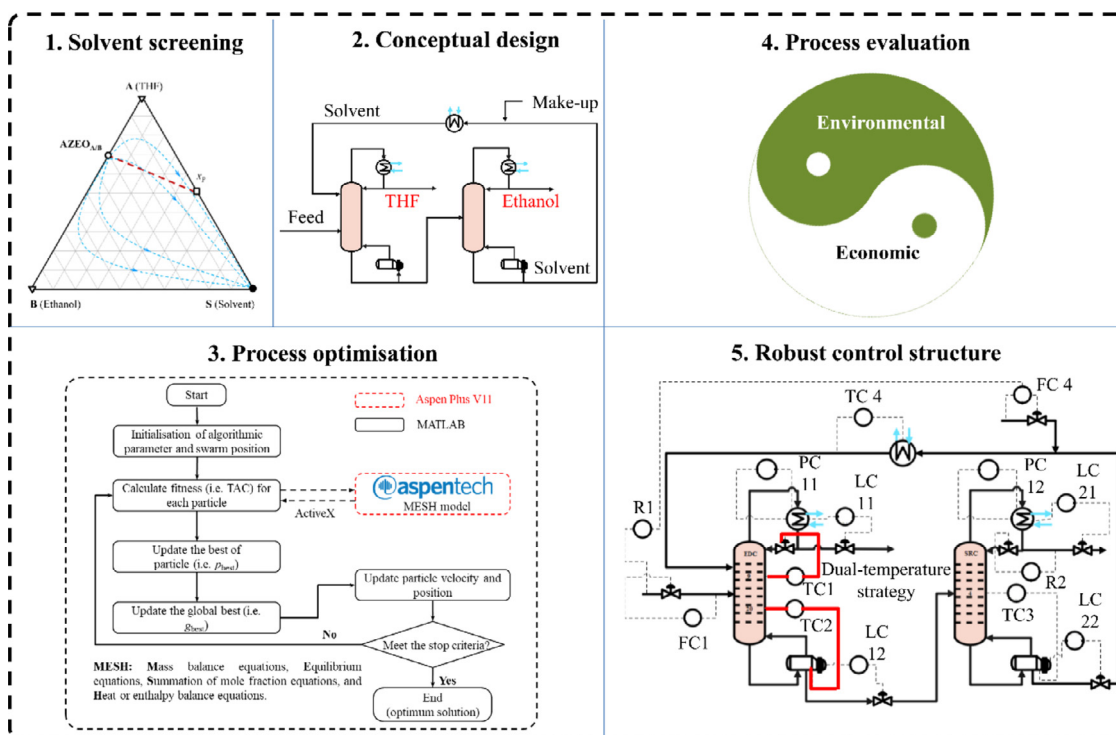


Fig. 3. Methodology for developing ED using DMSO employed in this work.

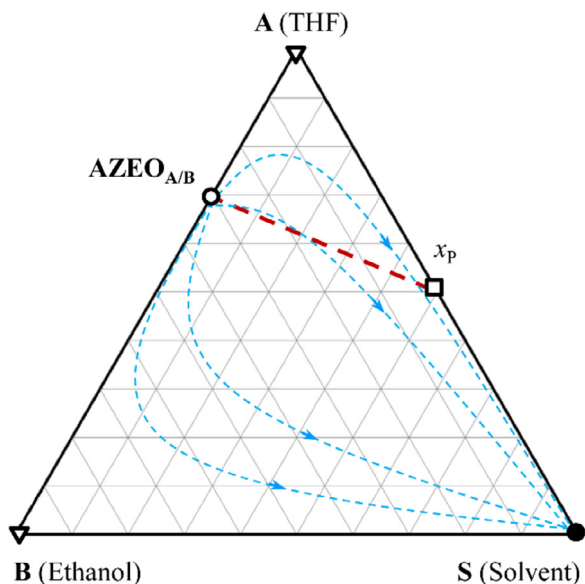


Fig. 4. Ternary diagram for binary azeotropic mixture with uni-volatility line (Serafimov's class 1.0 – 1a).

3.3. Process optimisation

In this section, the conceptual design from Section 3.2 is optimised to obtain the optimal configuration for improving the separation process performance. The proposed process in this study contains different discrete and continuous decision variables, which forms a mixed integer nonlinear programming problem (MINLP) that is difficult to handled by using the conventional sequential iterative (SI) or sequential quadratic programming (SQP) algorithm (Yang et al., 2022b). To overcome this issue, various stochastic optimisation algorithms can be employed such as genetic algorithm (GA) (Sun et al., 2020), mesh adaptive direct search

(MADS) algorithm (Li et al., 2020; Yang et al., 2022b), particle swarm optimisation (PSO) (Yang et al., 2022c), and simulated annealing (SA) algorithm (Yang and Ward, 2018). Among the different optimisation algorithm, PSO has a shorter computational times, which makes it a very popular approach for optimising advanced distillation-based processes (e.g. ED and RED) (Kong et al., 2022c; Yang et al., 2023). Therefore, PSO is used in this work for solving the MINLP problem, given by:

$$\min_{x \in R} f(x) = \text{TAC}$$

$$R = \{d \text{ \& } c\}$$

$$\text{Subject to } \{P_i \geq P^{\text{desired}}, i = 1, 2, \dots, n\} \quad (1)$$

The optimisation objective, $f(x)$, is to minimise the TAC at a restricted products purity specification (P^{desired}). The d and c represents the discrete and continuous decision variable, respectively. The design variables used for optimisation are similar to those listed in Section 3.2, including the initial values that were used for the optimisation. The ActiveX technique is employed in this study to link the TAC (i.e. objective function), purities constraint, design variables, and initial values in Aspen Plus with the optimisation algorithm in MATLAB (You et al., 2018) and the overall optimisation methodology is graphically represented by Fig. 5. The parameters of the PSO algorithm is given in Table S2.

Initially, the particle swarm parameter and position are generated arbitrarily using real numbers within the pre-defined constraint and then the fitness of each particle is calculated based on economic objective function (i.e. TAC). The best individual (p_{best}) and global (g_{best}) solution are updated based on two different situations, i.e. when the TAC of the present particle is lower than that of the previous particle, or when less than half of the individual solution did not overrule each other. The optimisation stops when the difference between consecutive objective function values is lower than 10^{-4} (i.e. stop criteria is met), else, the position and velocity of each particle will be updated.

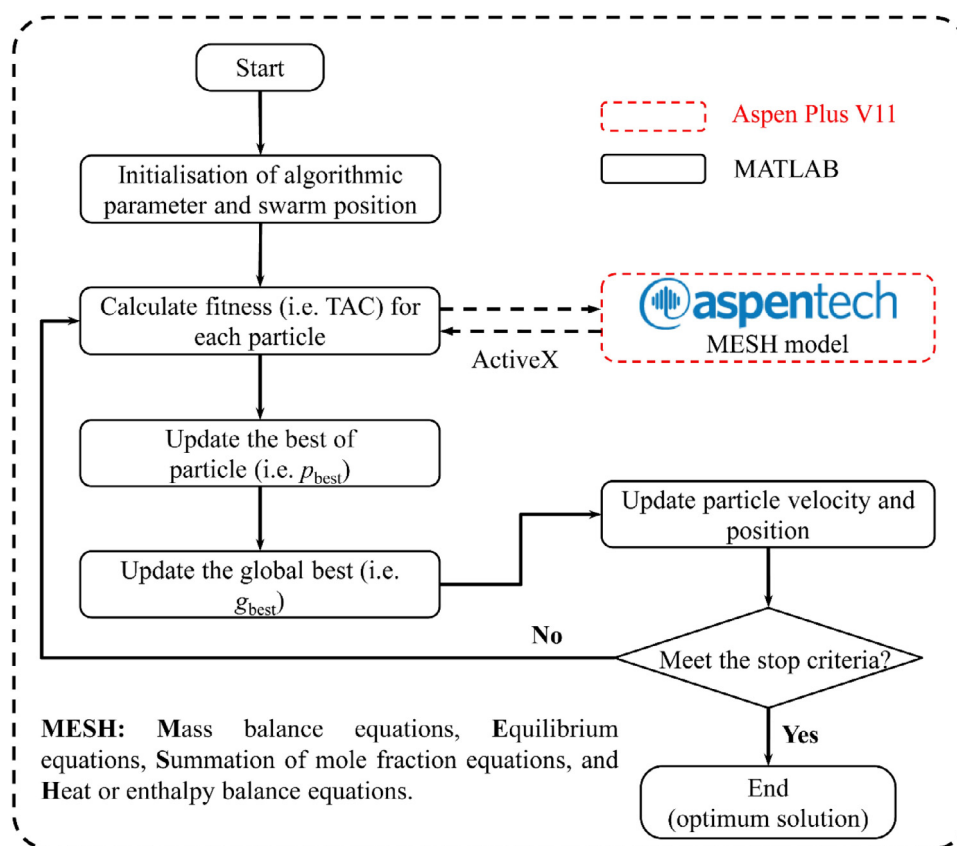


Fig. 5. The procedure of PSO algorithm employed in this work.

3.4. Process evaluation

The performance of our proposed process is examined based on TAC and CO₂ emission which represents the economic and environmental aspects.

3.4.1. Economic evaluation

The TAC is calculated by using Eq. (2).

$$\text{TAC} = \frac{\text{TCC}}{\text{PP}} + \text{TOC} \quad (2)$$

The TCC here refers to the total capital cost which includes the cost of all major equipment in the process such as the distillation tower, reboiler, condenser, and cooler. The TOC, on the other hand, is the total operational cost that accounts for the cost of different heating and cooling utilities such as pressurised steam and cooling water costs. PP is the payback period of 3 years. Fig. S1 graphically illustrated all the relevant equations used for assessing the TCC and TOC of the proposed process that were obtained from Douglas' textbook (Douglas, 1988).

3.4.2. Environmental evaluation

Other than economic evaluation, we also investigated the environmental performance of the ED using alternative solvent and compared it against previous work. Note that the environmental performance evaluation was not covered in the work of Wang et al. (2015a). Here, CO₂ emission that are generated from the external utilities such as boilers and furnace used for steam generation, are used to represent the environmental emission and it can be calculated using the reboiler energy consumption, similar to method employed by existing study (Yang et al., 2022b), given as:

$$(\text{CO}_2)_{\text{emission}} = \left(\frac{Q_{\text{fuel}}}{\text{NHV}} \times \frac{C}{100} \right) \alpha \quad (3)$$

Here, Eq. (4) is used to estimate the consumption of fuel (Q_{fuel}); α is the ratio of molecular weight of CO₂ to carbon; NHV is the net-heating value of 39,881 kJ kg⁻¹; and C is the carbon content, respectively.

$$Q_{\text{fuel}} = \frac{Q_p}{h_s} (E_s - 419) \times \frac{T_f - T_0}{T_f - T_s} \quad (4)$$

The Q_p here refers to the energy consumed by the reboilers in the process (kJ hr⁻¹); h_s and E_s are the latent heat of steam and enthalpy of the steam, respectively (kJ kg⁻¹). The T_f , T_s , and T_0 refers to the flame, stack, and ambient temperatures, respectively. These parameters are obtained from previous study by Su et al. (2020).

3.5. Dynamic simulation of the SSED

The steady-state simulation of the proposed ED is converted dynamic simulation via pressure-driven simulation in Aspen Plus. Prior to the conversion, all the equipment is sized accordingly. The diameter of the column tray and pressure drop are determined by Aspen Plus. The tray spacing is 0.6096 m while the weir height used for both EDC and SRC is 0.1016 m. The volume of the column base and reflux drum were assumed to be half-filled and have a 10-min holdup time. Once the ED has been successfully converted to Aspen Plus Dynamics, the inventory control loops are installed as illustrated in Fig. S2. The distillate and bottom flowrate are manipulated to maintain the level of the reflux drums and bottom of the columns, respectively. The condenser duty is used to control the pressure of the condenser for both columns. The fresh feed and solvent flowrate entering the columns are flow controlled. A flow ratio is additionally implemented to maintain the solvent to fresh feed flowrate. Lastly, the cooler temperature for solvent is controlled by using the cooler duty.

Other than inventory control, the quality control loop is also essential to maintain the products purities. Contrary to the ED using EG from

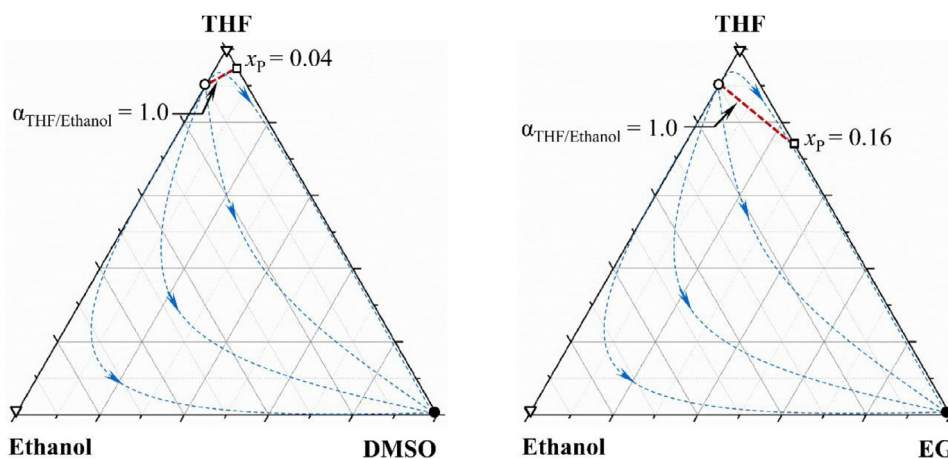


Fig. 6. Residue curve map(s) comparison for the binary azeotropic mixture containing THF and ethanol using DMSO and EG as solvent.

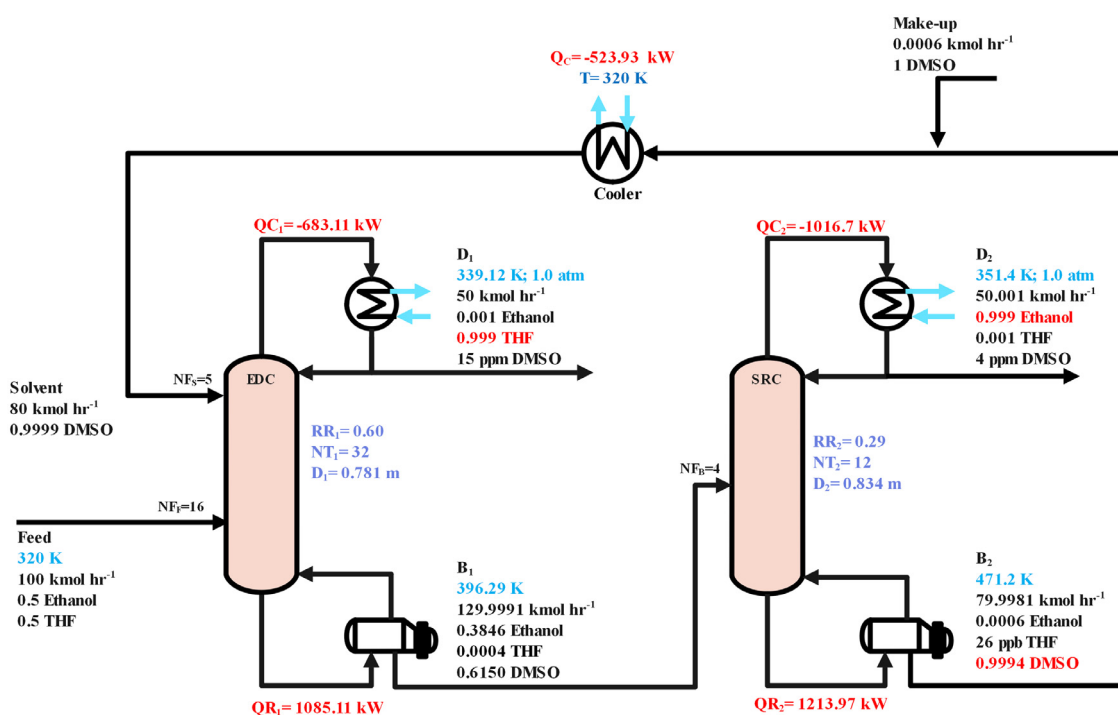


Fig. 7. Conceptual design for ED using DMSO.

previous study (Wang et al., 2015b), we intend to limit ourselves to the usage of only the temperature controller because the composition controller is less preferred in the industry due to its high prices and difficulty in maintenance. Before installing the temperature controller, it is necessary to determine the temperature-sensitive tray in both the EDC and SRC. Today, several techniques have been devised to determine the temperature-sensitive tray location such as slope criterion (Li et al., 2013), open-loop sensitivity analysis (Arifin and Chien, 2008), or using singular value decomposition (SVD) analysis (Zhang et al., 2021a), with each technique demonstrating its own distinct feature. In this work, we used the open-loop sensitivity analysis to locate the temperature-sensitive stage. The open-loop sensitivity analysis was conducted by applying a little change (e.g. $\pm 0.1\%$) to the manipulating variables (e.g. reboiler duty or reflux ratio) in the EDC and SRC. The stage(s) with the highest ΔT (i.e. changes in temperature) is identified as the temperature-sensitive stage. The relative gain array (RGA) analysis is employed to determine the best controller combination when the specific column con-

tains two or more temperature-sensitive stage. Internal model control (IMC) tuning rule is used to tune all the temperature controllers in this study. After all the controllers are installed, the control performance of the proposed process is tested by using $\pm 10\%$ throughput and $\pm 5\%$ feed composition disturbances.

4. Result and discussion

4.1. Steady-state simulation

4.1.1. Solvent screening

Fig. 6 shows the residue curve map(s) comparison for the binary mixture containing THF and ethanol using EG and DMSO as solvent. From Fig. 6, it appears that using DMSO provides the smallest x_p value, which reflect its superiority over using EG as solvent for the separation of THF and ethanol. Therefore, DMSO is employed as solvent in the ED for subsequent simulation.

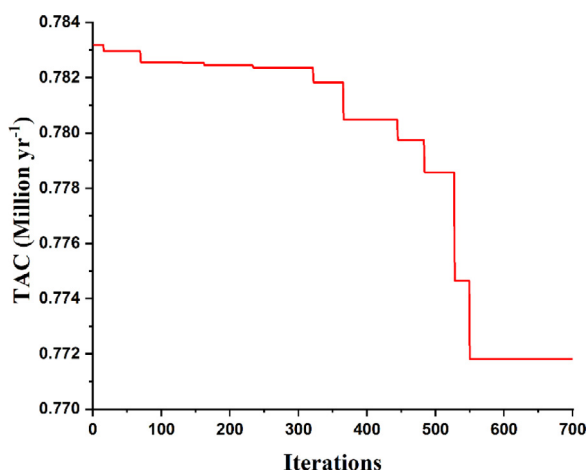


Fig. 8. Optimisation results for the proposed ED using DMSO as solvent.

4.1.2. Conceptual design

The conceptual design for the ED using DMSO is given by Fig. 7. The total energy consumption of the conceptual ED using DMSO was found to be 2299 kW, which represent 37% reduction in comparison to the ED using EG from previous work (Wang et al., 2015a). Such reduction in the energy consumption decreases the TOC as less amount of heating utilities is required, subsequently translate to 35% decrease in the TAC (i.e. from \$ 1.19 million to \$ 0.78 million) relative to previous work. Note that there is no significant difference caused by the difference in steam heating utility as the proposed ED using DMSO employed the same steam grade as the ED using EG from previous work. Other than that, the decrease in TAC can also be attributed to the decrease in TCC where the total number of stages for the EDC decrease by more than half from 70 stages to 32 stages in the proposed ED using DMSO. Then, the proposed ED using DMSO provides 37% lower CO₂ emission from 1239 kg hr⁻¹ to 777 kg hr⁻¹ relative to the ED using EG from previous work. It should be noted that the magnitude differences in the CO₂ emission and the energy consumption are analogous,

Table 1

TAC comparison between ED using DMSO (this work) against ED using EG and PSD (literature).

Parameters	Previous work		This work
	ED using EG	PSD	ED using DMSO
Total reboiler duty (kW)	3658	3087	2303 (-37% / -25%) ¹
TAC (\$ Million yr ⁻¹)	1.1978	1.014	0.77 (-36% / -24%) ¹
CO ₂ emission (kg hr ⁻¹)	1236	1044	779 (-37% / -25%) ¹

¹ Percentage difference between (ED using DMSO against ED using EG / ED using DMSO against PSD).

and this is because the CO₂ emission are almost directly proportional to the total energy consumption (Eq. (3)). In essence, a lower total energy consumption generally signifies a lower CO₂ emission.

4.1.3. Optimised design

The optimisation results for the proposed ED using DMSO is given by Fig. 8, with the optimised flowsheet displayed in Fig. 9. The total duration taken for the optimisation process is about 30 h using Intel (R) Core™ i7-9700 CPU @ 3.00 GHz and 16 GB memory. After optimisation, the total number of stages, solvent feed stage, and fresh feed stage in the EDC (Fig. 9) changed marginally in comparison to the conceptual design (Fig. 7). As for the SRC, the total number of stages decreased from 12 stages to 8 stages in the optimised design (Fig. 9) while the feed location of the SRC in the optimised process remained identical to the conceptual design.

From Fig. 8, it is apparent that the TAC becomes constant at about \$ 0.7718 million after about 550 iterations, which is about 1% lower than the initial design (Fig. 7) in Section 4.1.2. The total simulation run is 700 iterations. The total energy consumed by the optimised process however is similar to the conceptual design, despite by a higher extent of about 3 kW. Likewise, similar result was obtained for the CO₂ emission where the optimised ED provides identical performance relative to the ED using EG from previous work.

Altogether, the optimised ED using DMSO provides 37% decrease in both the energy and the CO₂ emission relative to the ED using EG from previous work (Table 1). The TAC for the optimised ED using DMSO

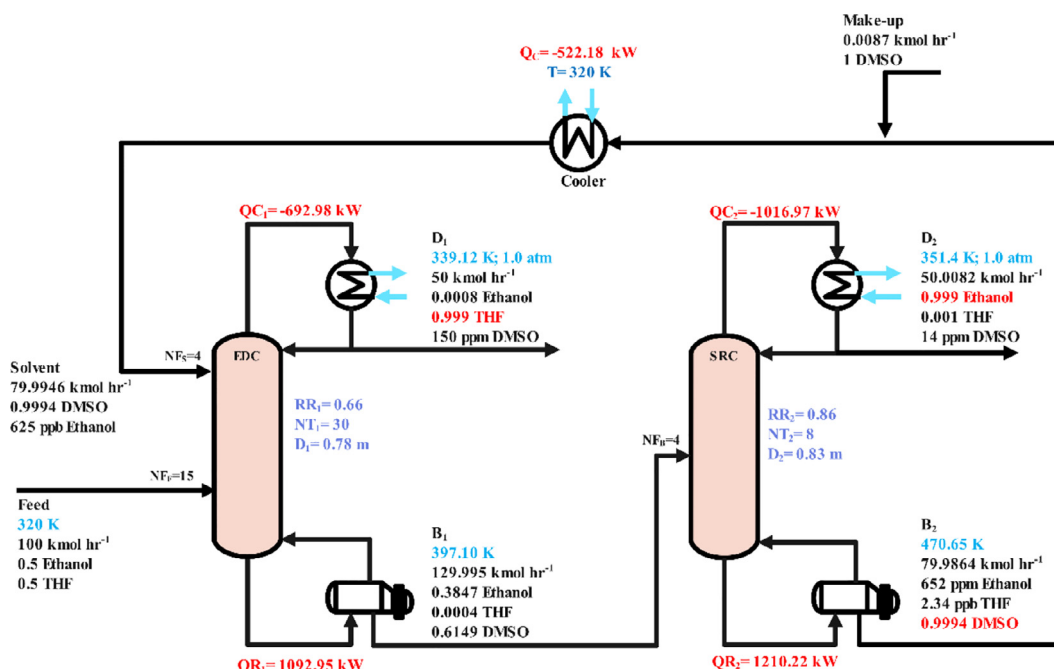


Fig. 9. Optimum column configuration for the proposed ED using DMSO as solvent.

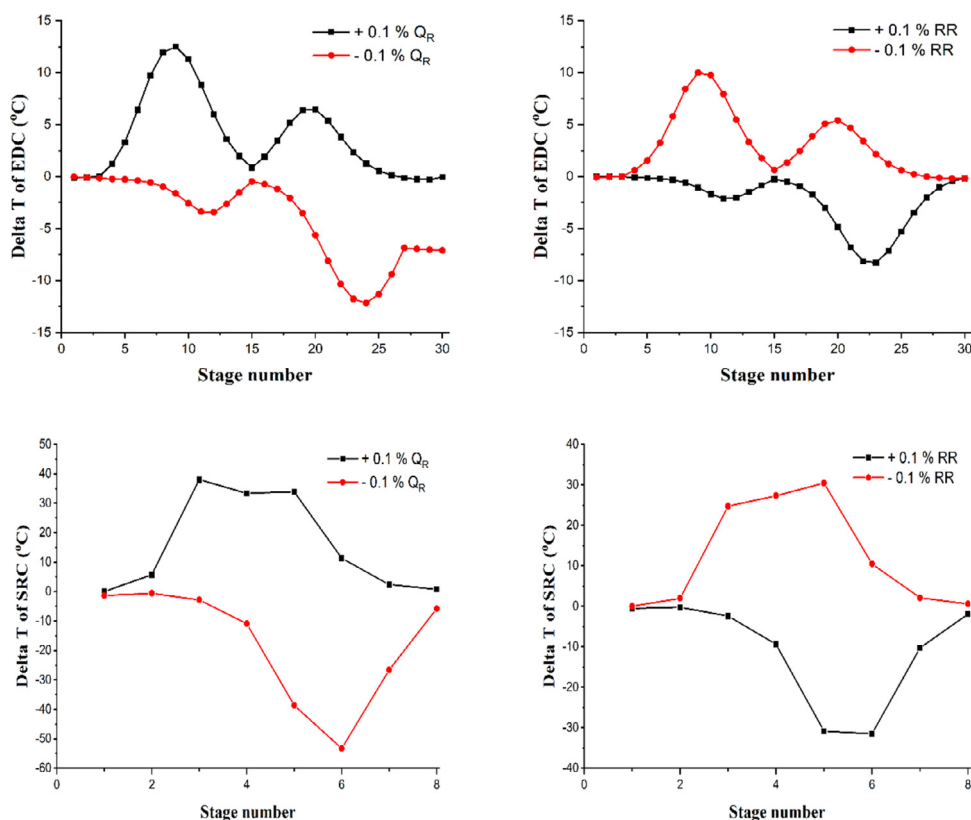


Fig. 10. Open-loop sensitivity analysis for the ED using DMSO with $\pm 0.1\%$ reboiler duty and reflux ratio.

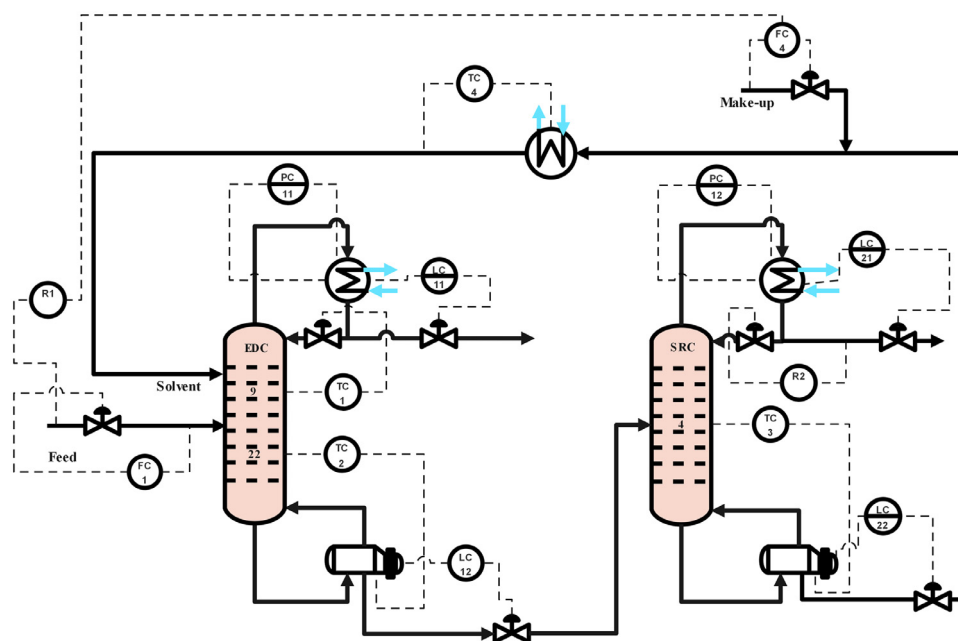


Fig. 11. Proposed dual-temperature control structure for ED using DMSO.

also reduced significantly by about 36% from \$ 1.197 million to \$ 0.771 million with respect to the ED using EG from previous work (Table 1).

In addition to the ED using EG, we also benchmark our proposed process against the PSD from previous work (Fig. S3) (Wang et al., 2015a) since it is the most economical process (i.e. best process) as demonstrated in previous work. Upon meticulous comparison, it becomes clear

that the proposed ED using DMSO provides 25% reduction in the total energy consumption and CO₂ emission. Another interesting observation was that the high-pressure column of the PSD from previous work only required medium-pressure steam as heating utility whereas the ED using DMSO proposed in this work employed high-pressure steam in the SRC, which provides substantial increase in the unit price for the heat-

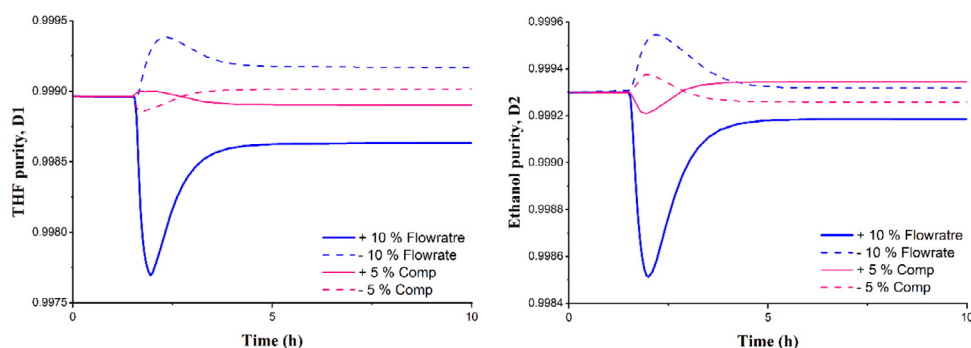


Fig. 12. Products purities under $\pm 10\%$ throughput and $\pm 5\%$ composition disturbances.

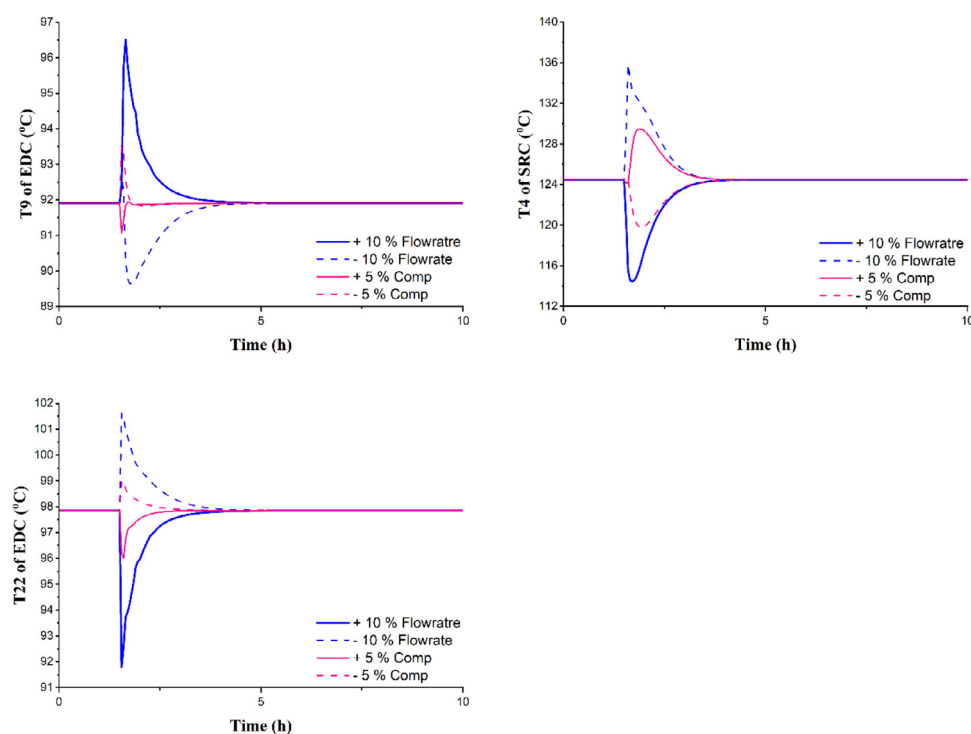


Fig. 13. Tray temperature under $\pm 10\%$ throughput and $\pm 5\%$ composition disturbances.

ing utility by 20% from \$ 8.22 per GJ to \$ 9.88 per GJ. Note that the TOC depends on both the reboiler energy consumption and the steam unit price and in the present case, the decrease in the total energy consumption is much larger than the increase in the steam unit price and therefore, the proposed ED using DMSO provides a net reduction in the TOC. In terms of column configuration, it was revealed that the optimised ED using DMSO has less total number of stages for both column, which provides significant decrease in the TCC. Altogether, the TAC of the optimised ED using DMSO is lower than the PSD (i.e. best process) from previous work by about 24%.

Here, it is worth noting that although both the PSD and ED from previous work have been optimised to their minimum TAC, the optimisation algorithm used is different from this work that relied on PSO, which may affect the result comparison. Nonetheless, we believe that the difference would be marginal because it has been shown in Section 4.1.2 that the conceptual design of our proposed process (i.e. ED using DMSO) is already significantly better than that of the ED from previous work by about 37%, 35%, and 37% in energy, TAC and CO_2 emission, respectively, prior to optimisation.

4.2. Dynamic simulation

The results of the open-loop sensitivity analysis for the ED using DMSO is depicted in Fig. 10.

It appears that the EDC has two temperature-sensitive regions (Fig. 10). The first region is in between stage 3 to stage 12 while the second region is located below stage 12 (i.e. stage 12 to stage 30). In the first region, stage 9 displayed the highest change in temperature and therefore is selected as the first control point. As for the second region, both positive and negative changes to the reboiler duty and reflux ratio correspond to an asymmetric profile. It was observed that stage 20 and stage 24 displayed the highest changes in temperature (Fig. 10) and to seek balance between both stages, stage 22 was selected as a middle point for the temperature control using reboiler duty. If the products purities under both throughput and feed composition is unacceptable, a more complicated control structure such as dual temperature control or average temperature control would have to be used. The usage of composition controller to manipulate the solvent-to-feed ratio as in the case of previous work can also be considered. To further support the re-

liability of such pairing, RGA analysis was conducted and results shows that stage 9 should be paired with reflux ratio and stage 22 should be paired with reboiler duty. For the SRC, there is only one sensitive tray temperature and therefore, we decided to control it using the reboiler duty while the reflux ratio is fixed at their steady-state value. The resulting proposed control structure for the proposed ED using DMSO is given in Fig. 11. The effectiveness of the control structure is tested in using $\pm 10\%$ throughput and $\pm 5\%$ composition disturbances and the results are displayed in Figs. 12 and 13.

From Figs. 12 and 13, all the purities returned to a value close the original setpoint of 99.9 mol.% under both throughput and feed composition disturbances in less than 3 h, which reflects the effectiveness of the proposed control structure. The largest offset occurred in the THF purity where it drops to 99.87 mol.% during the +10% throughput disturbance but such offset in our opinion was still within the acceptable range since the proposed control structure does not rely on any composition controller as in the case of previous work (Wang et al., 2015b). In terms of tray temperature control, the proposed control structure can return the temperature back to their desired values under 3 h, which again reflect the outstanding control performance of our proposed process. Here, one observation from Fig. 13 worth pointing out was that there is a drop in tray temperature at the bottom of the EDC (i.e. stage 22) and SRC (i.e. stage 4) during the +10% throughput disturbance, which affects the products purities substantially. To maintain the products purities at their desired specification under positive throughput disturbance, the reboiler heat duty must be increased, and this can be performed through the temperature controller. On the other hand, the reboiler temperature must be reduced when there is negative throughput disturbance because such disturbance increases the tray temperature at the bottom that affects the products purities. For the same reason, similar observation was made for the tray temperature on top of the EDC (i.e. stage 9), although the tray temperature for column top showed a symmetrical performance relative to the column bottom. Similar observations were seen when the system is subjected to both positive and negative feed composition disturbances. Overall, the control structure is considerably effective since it can withhold the product purities and temperature very close to their desired value under minimum transient time.

5. Conclusion

In conclusion, we revisited the ED using EG proposed by previous work for the recovery of binary azeotropic mixture containing THF and ethanol and proposed the usage of DMSO as an alternative solvent to improve the economic, environmental, and control performance. The suitability of the DMSO as an alternative solvent was preliminary screened and compared against using EG from previous work using the residue curve map(s). Then, the ED using DMSO was conceptually design by manipulating all the design variables until the minimum product specifications (i.e. purity) are achieved. The proposed design is further optimised using PSO to obtain the optimal flowsheet and the performance is compared against using EG from previous work based on the TAC and CO₂ emission. Overall, the optimised ED using DMSO provides 36% and 37% lower TAC and CO₂ emission in comparison to the ED using EG from previous work. In addition, we also benchmark the proposed ED using DMSO against the PSD from previous work and concluded that the proposed process provides 24% and 25% lower TAC and CO₂ emission with respect to the PSD (i.e. best process) from previous work. Other than steady-state simulation, we also developed a control structure that is capable of handling $\pm 10\%$ throughput and $\pm 5\%$ feed composition disturbances. The proposed control structure in the present work which rely solely on the temperature controller is considerably effective in maintaining the products purities and tray temperature of the columns in comparison to the control structure for the ED using EG from previous work, which required the usage of the composition controller. To further enhance the performance of the separation process and reduce the

energy consumption, we recommend to explore on the potential application of energy intensified processes for the proposed ED using DMSO in the future.

Acknowledgement

Zong Yang Kong and Jaka Sunarso gratefully acknowledged the support from Swinburne University of Technology Sarawak Campus.

Supplementary materials

Supplementary material associated with this article can be found, in the online version, at doi:10.1016/j.dche.2022.100060.

References

- Alcántara Avila, J.R., Kong, Z.Y., Lee, H.Y., Sunarso, J., 2021. Advancements in optimization and control techniques for intensifying processes. *Processes* doi:10.3390/pr9122150.
- Arifin, S., Chien, I.L., 2008. Design and control of an isopropyl alcohol dehydration process via extractive distillation using dimethyl sulfoxide as an entrainer. *Ind. Eng. Chem. Res.* 47, 790–803. doi:10.1021/ie070996n.
- Chen, Y.Y., Kong, Z.Y., Yang, A., Lee, H.Y., Sunarso, J., 2022. Design and control of an energy intensified side-stream extractive distillation for binary azeotropic separation of n-hexane and ethyl acetate. *Sep. Purif. Technol.* 294, 121176. doi:10.1016/j.seppur.2022.121176.
- Douglas, J.M., 1988. *Conceptual Design of Chemical Processes*. McGraw-Hill.
- Gerbaud, V., Rodríguez-Donis, I., Hegely, L., Lang, P., Denes, F., You, X., 2019. Review of extractive distillation. *Process design, operation, optimization and control*. *Chem. Eng. Res. Des.* 141, 229–271. doi:10.1016/j.cherd.2018.09.020.
- Kong, Z.Y., Lee, H.Y., Sunarso, J., 2022a. The evolution of process design and control for ternary azeotropic separation: recent advances in distillation and future directions. *Sep. Purif. Technol.* doi:10.1016/j.seppur.2021.120292.
- Kong, Z.Y., Sunarso, J., Yang, A., 2022b. Recent progress on hybrid reactive-extractive distillation for azeotropic separation: a short review. *Front. Chem. Eng.* 4.
- Kong, Z.Y., Yang, A., Chua, J., Chew, J.J., Sunarso, J., 2022c. Energy-efficient hybrid reactive-extractive distillation with a preconcentration column for recovering isopropyl alcohol and diisopropyl ether from wastewater: process design, optimization, and intensification. *Ind. Eng. Chem. Res.* 61, 11156–11167. doi:10.1021/acs.iecr.2c01768.
- Li, J., Li, R., Zhou, H., Yang, X., Ma, Z., Sun, L., Zhang, N., 2019. Energy-saving ionic liquid-based extractive distillation configurations for separating ternary azeotropic system of tetrahydrofuran/ethanol/water. *Ind. Eng. Chem. Res.* 58, 16858–16868. doi:10.1021/acs.iecr.9b02141.
- Li, Q., Feng, Z., Rangaiah, G.P., Dong, L., 2020. Process optimization of heat-integrated extractive dividing-wall columns for energy-saving separation of CO₂ and hydrocarbons. *Ind. Eng. Chem. Res.* 59, 11000–11011. doi:10.1021/acs.iecr.0c00666.
- Li, W., Shi, L., Yu, B., Xia, M., Luo, J., Shi, H., Xu, C., 2013. New pressure-swing distillation for separating pressure-insensitive maximum boiling azeotrope via introducing a heavy entrainer: design and control. *Ind. Eng. Chem. Res.* 52, 7836–7853. doi:10.1021/ie400274d.
- Luis, P., Amelio, A., Vreysen, S., Calabro, V., van der Bruggen, B., 2014. Simulation and environmental evaluation of process design: distillation vs. hybrid distillation-pervaporation for methanol/tetrahydrofuran separation. *Appl. Energy* 113, 565–575. doi:10.1016/j.apenergy.2013.06.040.
- Su, Y., Yang, A., Jin, S., Shen, W., Cui, P., Ren, J., 2020. Investigation on ternary system tetrahydrofuran/ethanol/water with three azeotropes separation via the combination of reactive and extractive distillation. *J. Clean. Prod.* 273, 123145. doi:10.1016/j.jclepro.2020.123145.
- Sun, S., Chun, W., Yang, A., Shen, W., Cui, P., Ren, J., 2020. The separation of ternary azeotropic mixture: thermodynamic insight and improved multi-objective optimization. *Energy* 206, 118117. doi:10.1016/j.energy.2020.118117.
- Tang, K., Bai, P., Huang, C., Liu, W., 2013. Separation of tetrahydrofuran-ethanol azeotropic mixture by extractive distillation. *Asian J. Chem.* 25, 2774–2778. doi:10.14233/ajchem.2013.13870.
- Wang, Q., Yu, B., Xu, C., 2012. Design and control of distillation system for methylal/methanol separation. Part 1 : extractive distillation using DMF as an entrainer. *Ind. Eng. Chem. Res.* 51, 1281–1292. doi:10.1021/ie201946d.
- Wang, Y., Cui, P., Ma, Y., Zhang, Z., 2015a. Extractive distillation and pressure-swing distillation for THF/ethanol separation. *J. Chem. Technol. Biotechnol.* 90, 1463–1472. doi:10.1002/jctb.4452.
- Wang, Y., Zhang, Z., Zhao, Y., Liang, S., Bu, G., 2015b. Control of extractive distillation and partially heat-integrated pressure-swing distillation for separating azeotropic mixture of ethanol and tetrahydrofuran. *Ind. Eng. Chem. Res.* 54, 8533–8545. doi:10.1021/acs.iecr.5b01642.
- Yang, A., Kong, Z.Y., Sunarso, J., 2023. Design and optimisation of novel hybrid side-stream reactive-extractive distillation for recovery of isopropyl alcohol and ethyl acetate from wastewater. *Chem. Eng. J.* 451, 138563. doi:10.1016/j.cej.2022.138563.
- Yang, A., Kong, Z.Y., Sunarso, J., Shen, W., 2022a. Towards energy saving and carbon reduction of pressure-swing distillation for separating the ternary azeotropic mix-

- tures by thermodynamic insights and process intensification. *Sep. Purif. Technol.* 301, 121983. doi:10.1016/j.seppur.2022.121983.
- Yang, A., Kong, Z.Y., Sunarso, J., Su, Y., Wang, Q., Zhu, S., 2022b. Insights on sustainable separation of ternary azeotropic mixture tetrahydrofuran/ethyl acetate/water using hybrid vapor recompression assisted side-stream extractive distillation. *Sep. Purif. Technol.* 290, 1383–5866. doi:10.1016/j.seppur.2022.120884.
- Yang, A., Shen, W., Wei, S., Dong, L., Li, J., Gerbaud, V., 2019. Design and control of pressure-swing distillation for separating ternary systems with three binary minimum azeotropes. *AIChE J.* 65, 1281–1293. doi:10.1002/aic.16526.
- Yang, A., Su, Y., Sun, S., Shen, W., Bai, M., Ren, J., 2022c. Towards sustainable separation of the ternary azeotropic mixture based on the intensified reactive-extractive distillation configurations and multi-objective particle swarm optimization. *J. Clean. Prod.* 332. doi:10.1016/j.jclepro.2021.130116.
- Yang, A., Su, Y., Teng, L., Jin, S., Zhou, T., Shen, W., 2020. Investigation of energy-efficient and sustainable reactive/pressure swing distillation processes to recover tetrahydrofuran and ethanol from the industrial effluent. *Sep. Purif. Technol.* doi:10.1016/j.seppur.2020.117210.
- Yang, X., Ward, J.D., 2018. Extractive distillation optimization using simulated annealing and a process simulation automation server. *Ind. Eng. Chem. Res.* 57, 11050–11060. doi:10.1021/acs.iecr.8b00711.
- You, X., Gu, J., Gerbaud, V., Peng, C., Liu, H., 2018. Optimization of pre-concentration, entrainer recycle and pressure selection for the extractive distillation of acetonitrile-water with ethylene glycol. *Chem. Eng. Sci.* 177, 354–368. doi:10.1016/j.ces.2017.11.035.
- Zhang, Q., Hou, W., Ma, Y., Yuan, X., Zeng, A., 2021a. Dynamic control analysis of eco-efficient double side-stream ternary extractive distillation process. *Comput. Chem. Eng.* 147, 107232. doi:10.1016/j.compchemeng.2021.107232.
- Zhang, Q., Zeng, A., Yuan, X., Ma, Y., 2019. Control comparison of conventional and thermally coupled ternary extractive distillation processes with recycle splitting using a mixed entrainer as separating agent. *Sep. Purif. Technol.* 224, 70–84. doi:10.1016/j.seppur.2019.04.085.
- Zhang, X., Zhao, Y., Wang, H., Qin, B., Zhu, Z., Zhang, N., Wang, Y., 2018. Control of a ternary extractive distillation process with recycle splitting using a mixed entrainer. *Ind. Eng. Chem. Res.* 57, 339–351. doi:10.1021/acs.iecr.7b04071.
- Zhang, Y.R., Wu, T.W., Chien, I.L., 2021b. Intensified hybrid reactive-extractive distillation process for the separation of water-containing ternary mixtures. *Sep. Purif. Technol.* 279. doi:10.1016/j.seppur.2021.119712.
- Zhao, Y., Jia, H., Geng, X., Wen, G., Zhu, Z., Wang, Y., 2017a. Comparison of conventional extractive distillation and heat integrated extractive distillation for separating tetrahydrofuran/ethanol/water. *Chem. Eng. Trans.* 61, 751–756. doi:10.3303/CET1761123.
- Zhao, Y., Ma, K., Bai, W., Du, D., Zhu, Z., Wang, Y., Gao, J., 2018. Energy-saving thermally coupled ternary extractive distillation process by combining with mixed entrainer for separating ternary mixture containing bioethanol. *Energy* 148, 296–308. doi:10.1016/j.energy.2018.01.161.
- Zhao, Y., Zhao, T., Jia, H., Li, X., Zhu, Z., Wang, Y., 2017b. Optimization of the composition of mixed entrainer for economic extractive distillation process in view of the separation of tetrahydrofuran/ethanol/water ternary azeotrope. *J. Chem. Technol. Biotechnol.* 92, 2433–2444. doi:10.1002/jctb.5254.